THE JOURNAL OF PHYSICAL CHEMISTRY B

Article

pubs.acs.org/JPCB

Structure and Dynamics of 1-*N*-Alkyl-3-*N*-Methylimidazolium Tetrafluoroborate + Acetonitrile Mixtures

Alexander Stoppa,[†] Johannes Hunger,[†] Glenn Hefter,[‡] and Richard Buchner*,[†]

[†]Institut für Physikalische und Theoretische Chemie, Universität Regensburg, D-93040 Regensburg, Germany

[‡]Chemistry Department, Murdoch University, Murdoch, WA 6150, Australia

Supporting Information

ABSTRACT: A detailed investigation of the binary mixtures of the ionic liquids (ILs) 1-*N*-R-3-*N*-methylimidazolium tetrafluoroborate (R = ethyl, *n*-butyl, *n*-hexyl) with the important molecular solvent acetonitrile (AN) over the entire composition range has been made at 25 °C using broadband dielectric spectroscopy. All spectra showed two modes: a Cole−Cole (CC) mode centered at ∼2 GHz and a Debye mode centered at ∼50 GHz. However, detailed analysis indicated both relaxations were composites. The Debye mode arises from the rotational diffusion of free AN molecules with contributions from ultrafast vibrations and librations of the ILs. The CC mode corresponds to the jump rotation of the imidazolium cations and the hindered rotational diffusion of "slow" AN molecules solvating them. At very low IL concentrations 1:1 contact ion pairs are dominant. Overall, these IL + AN mixtures can be divided into two broad regions: at IL mole fraction (x_{IL}) $\lesssim$ 0.2 the IL behaves as a rather weakly associated conventional electrolyte while at $x_{IL} \gtrsim 0.2$ it takes on its IL characteristics, "lubricated" by the AN.

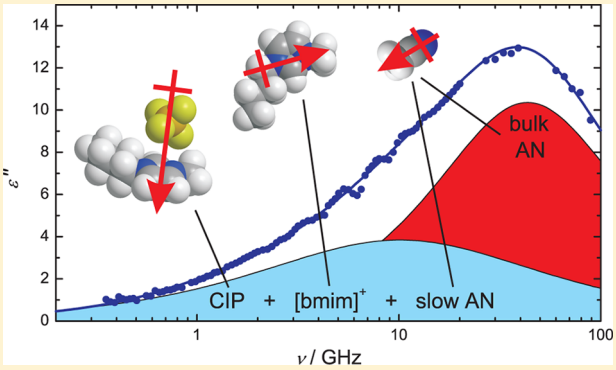

1. INTRODUCTION

The special properties of room temperature ionic liquids (ILs) and the resulting broad range of their potential applications is reflected in the vast number of publications on these substances that have appeared in recent years.[1−5] For most technological purposes, ILs will rarely be employed in neat form: almost invariably they will be diluted either by reactants and products or by the presence of a cosolvent, deliberately added to optimize their chemical and/or physical characteristics. However, up to now, relatively few systematic investigations of the structural and dynamical properties of mixtures of ILs with conventional molecular solvents have been reported;[6−13] and of these very few have covered the entire composition range.[6,7,9−12]

Acetonitrile (CH_3CN, AN) is an extremely versatile dipolar aprotic solvent that has been widely employed, for example, in the hydrometallurgical processing of Cu,[14] in battery applications,[15] and as a mobile phase in liquid chromatography.[16] Acetonitrile has a convenient liquid range, a reasonably high dielectric constant ($\varepsilon_{AN} \approx 36$ at 25 °C),[17] and the ability to dissolve a wide range of organic and inorganic compounds.[15,17,18] Of special relevance to the present work is that AN is known to be fully miscible with many alkylimidazolium-based ILs at ambient temperatures.[19,20]

The present study aims to investigate the structure and dynamics of mixtures of AN with some ILs, especially with regard to their variation with composition. The main technique chosen for this study was dielectric relaxation spectroscopy (DRS), which probes the fluctuations of the macroscopic dipole moment of a liquid in response to an applied oscillating electromagnetic field.[21] In the microwave (GHz) region, DRS is mainly sensitive to the reorientation of dipolar species and to collective intermolecular vibrations occurring on the pico- to nanosecond time scale.[22] DRS is especially sensitive to the presence of ion pairs,[22−24] which have often been invoked to explain various IL properties, such as their relatively low conductance and high viscosity,[25] even though the existence of such species has yet to be proven in most ILs.[12,26] DRS also yields information on solute−solvent interactions[22] and thus complements other techniques, like vibrational spectroscopy,[27] in solvation studies. An important feature of DRS is that it is the only technique providing access to the static permittivity of conducting samples, which is a required input for many theories. Furthermore, the dielectric relaxation behavior of solutions directly influences solvation dynamics and fast reaction kinetics therein.[28]

Accordingly, this paper reports a detailed DRS investigation over the entire composition range of the binary mixtures of 1-*N*-alkyl-3-*N*-methylimidazolium tetrafluoroborate salts ([Rmim][BF_4]), where R = e(thyl), b(utyl), or h(exyl) with AN, over the frequency range 0.2 $\leq \nu$/GHz $\leq$ 89 at 25 °C. Tetrafluoroborate salts were selected, despite their tendency to

Received: March 2, 2012
Revised: May 16, 2012
Published: June 10, 2012

   dx.doi.org/10.1021/jp3020673 | *J. Phys. Chem. B* 2012, 116, 7509−7521

hydrolyze,[29] because they are either commercially available or easily prepared and purified, and because they are still frequently used in application-oriented studies. Additionally, because of its tetrahedral symmetry, BF_4^- has zero dipole moment and thus makes no direct contribution to the dielectric spectra, thereby simplifying their analysis.

2. EXPERIMENTAL SECTION

Materials. Neat [emim][BF_4] was purchased from IoLiTec (Denzlingen, Germany) while [bmim][BF_4] and [hmim][BF_4] were prepared by anion metathesis between equimolar amounts of the appropriate 1-*N*-alkyl-3-*N*-methylimidazolium chloride dissolved in dichloromethane and an aqueous solution of $NaBF_4$. Detailed synthetic and purification procedures, together with the purities and water contents of the derived samples are given elsewhere.[29] The hygroscopic ILs so obtained were stored in a nitrogen-filled glovebox. Acetonitrile (Merck ≥99.9%) was distilled from CaH_2 and stored over activated 4 Å molecular sieves (final GC purity >99.99%; water content <50 ppm).

Mixtures were prepared using an analytical balance without buoyancy corrections and thus were accurate to about ±0.2%. Solutions were transferred to the DRS apparatus using syringe techniques. Sample preparation, handling, and measurement were performed under dry N_2(g). Measurements were conducted as quickly as possible to minimize possible ingress of water and decomposition of BF_4^-.

Dielectric and Other Measurements. The quantity directly accessible in DRS is the total complex permittivity

$$\hat{\eta}(\nu) = \eta'(\nu) - i\eta''(\nu) \quad (1)$$

which is recorded as a function of frequency ν.[21,30] As measured, $\hat{\eta}(\nu)$ includes the time-dependent contributions, which are described by the complex permittivity: $\hat{\varepsilon}(\nu) = \varepsilon'(\nu) - i\varepsilon''(\nu)$, and also an Ohmic loss term characterized by the dc conductivity, κ, arising from the steady-state migration of the ions under the influence of the electromagnetic field. The relationship between these quantities is

$$\hat{\eta}(\nu) = \hat{\varepsilon}(\nu) - i\kappa/(2\pi\nu\varepsilon_0) \quad (2)$$

where ε_0 is the permittivity of free space. The (relative) permittivity, $\varepsilon'(\nu) = \eta'(\nu)$, and the dielectric loss, $\varepsilon''(\nu)$, refer to the polarization components that are respectively in-phase and out-of-phase with the applied field and thus monitor the dynamics of the sample. As noted previously,[31,32] because $\lim_{\nu\to 0}\varepsilon''(\nu) = 0$, reliable analysis of $\hat{\varepsilon}(\nu)$ for conducting samples at lower frequencies is restricted to $\nu \geq \nu_{min}$, which is usually taken to be the frequency at which $\varepsilon''/\Delta\eta'' < 1$, where $\Delta\eta''$ is the experimental uncertainty in η''.

For the present IL + AN mixtures DR spectra were measured in the frequency range $0.2 \leq \nu/\text{GHz} \leq 20$ using a Hewlett-Packard model HP 85070 M dielectric probe system. This consisted of a HP 8720D vector network analyzer (VNA) and a HP 85070 M dielectric probe kit.[33,34] The VNA probe was calibrated using air, mercury, and purified *N*,*N*-dimethylacetamide as primary calibration standards. Calibration errors were corrected with a complex Padé approximation,[35] using puified AN, benzonitrile, and 1-butanol as reference materials. Measurements were limited to $0.2 \leq \nu_{min}/\text{GHz} \lesssim 0.5$ (depending on composition) due to the relatively large dc conductivities. Higher-frequency data were obtained using two waveguide interferometers (IFMs) covering the range $27 \leq \nu/\text{GHz} \leq 89$.[36,37] Since IFMs do not require calibration, the reliability of the VNA measurements and their Padé correction was crosschecked for one sample with two additional IFMs operating at $8.5 \leq \nu/\text{GHz} \leq 17.5$. Excellent agreement was found between the VNA and IFM data (Figure S1, Supporting Information), with values being well within the estimated uncertainties of the instruments: ≲2% for $\varepsilon'(\nu)$ and ≲3% for $\varepsilon''(\nu)$. All VNA and IFM measurements were carried out at 25.00 ± 0.05 °C.

Complex permittivity spectra, $\hat{\varepsilon}(\nu)$, were obtained by subtracting the conductivity contribution from the measured $\hat{\eta}(\nu)$ values, eq 2. The value of κ for the mixtures can be determined, in principle, from conventional low-frequency conductance measurements[33] or as an additional parameter in the fitting of the DRS data. In practice, fitted κ values differ slightly from directly measured values due to field imperfections arising from the geometry of the VNA probe.[38] Accordingly, experimental dc conductivities[29] were chosen as a starting approximation in the fitting procedure and then adjusted to achieve the best fit. Spectra were rejected if the experimental and fitted κ values differed by more than 5%. Typical $\hat{\varepsilon}(\nu)$ spectra are shown in Figure 1 and in Figures S2 and S3 in the Supporting Information.

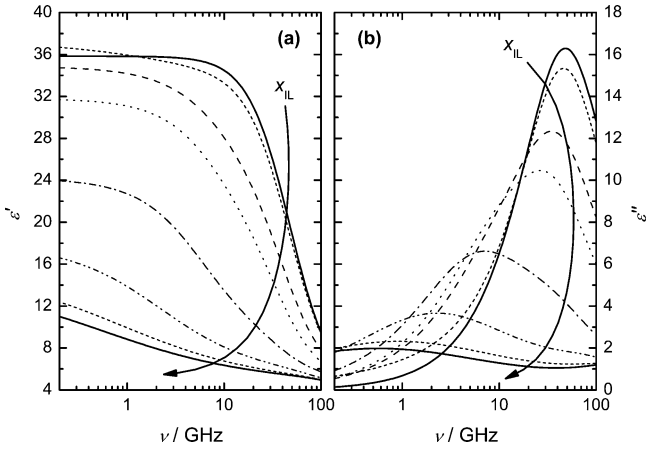

Figure 1. (a) Relative permittivity, $\varepsilon'(\nu)$, and (b) dielectric loss, $\varepsilon''(\nu)$, spectra of selected [bmim][BF_4] + AN mixtures at 25 °C. Arrows indicate increasing IL mole fraction (x_{IL} = 0, 0.05688, 0.1077, 0.2966, 0.6126, 0.8943, 1). Spectra of the neat components are indicated by the full lines.

Densities, ρ, electrical conductivities, κ, and molar conductivities, $\Lambda(= \kappa/c)$, of the present IL + AN mixtures at 25 °C, together with the experimental details, have been reported elsewhere.[29] Additional data for [bmim][BF_4] + AN mixtures obtained in this study are summarized in Table S1 in the Supporting Information. The estimated uncertainty for ρ is ±0.05 kg m^{-3}, while κ and Λ are thought to be accurate to ±0.5%.

3. DATA ANALYSIS

Dielectric spectra were described formally using all reasonable relaxation models, with up to five individual relaxation processes (n = 5 in eq 3). As input for the fit $\hat{\varepsilon}(\nu)$ was preferred over the dielectric modulus,[21] $\hat{M}(\nu) = 1/\hat{\eta}(\nu)$, as the latter unduly suppressed the low-frequency mode specific to the ILs. Each model was tested by simultaneously fitting $\varepsilon'(\nu)$ and $\varepsilon''(\nu)$ using a nonlinear least-squares routine based on the Levenberg–Marquardt algorithm. For all spectra each dispersion step j, characterized by an amplitude, S_j, and a

dx.doi.org/10.1021/jp3020673 | J. Phys. Chem. B 2012, 116, 7509–7521

relaxation time, τ_j, was modeled using the Havriliak–Negami (HN) equation

$$\hat{\varepsilon}(\nu) = \sum_{j=1}^{n} \frac{S_j}{[1 + (i2\pi\nu\tau_j)^{1-\alpha_j}]^{\beta_j}} + \varepsilon_\infty \quad (3)$$

with relaxation time distribution parameters $0 \leq \alpha_j < 1$ and $0 < \beta_j \leq 1$, or its simplified variants: the Cole–Davidson (CD, $\alpha_j = 0$), Cole–Cole (CC, $\beta_j = 1$), and Debye (D, $\alpha_j = 0$, $\beta_j = 1$) equations.[30,39] The various tested models were assessed according to the value χ_r^2 of their reduced error function,[40] systematic deviations between calculated and experimental $\hat{\varepsilon}(\nu)$, and the consistency of the parameters obtained over the entire composition range.

All of the IL + AN mixtures investigated were well fitted (Figure 2) by the superposition of just two processes: a low-frequency Cole–Cole mode ($j = 1$) and a higher-frequency Debye relaxation ($j = 2$). The parameters obtained for this CC +D model, together with the associated χ_r^2 values are summarized in Tables 1–3. For mixtures at IL mole fractions (x_{IL}) < 0.2, fits that included an additional low-frequency Debye process, i.e., a D+CC+D model, yielded χ_r^2 values (Tables S2–S4, Supporting Information) that were similar to the CC+D model. The implications of this finding are discussed in detail below. All other fit models, including those using a CD equation to model Kohlrausch stretched dynamics[21] for the IL, yielded larger χ_r^2 values and parameters that did not vary consistently with x_{IL}. Note that for the present spectra at $\nu \leq 89$ GHz the "infinite-frequency" permittivity, ε_∞, not only includes the intramolecular polarizability of the sample[30] but also contributions from any fast intermolecular modes (librations and intermolecular vibrations), which are significant for many neat ILs.[31,41] The static (relative) permittivity, ε, of the samples is given by $\varepsilon = \varepsilon_\infty + \sum S_j$.

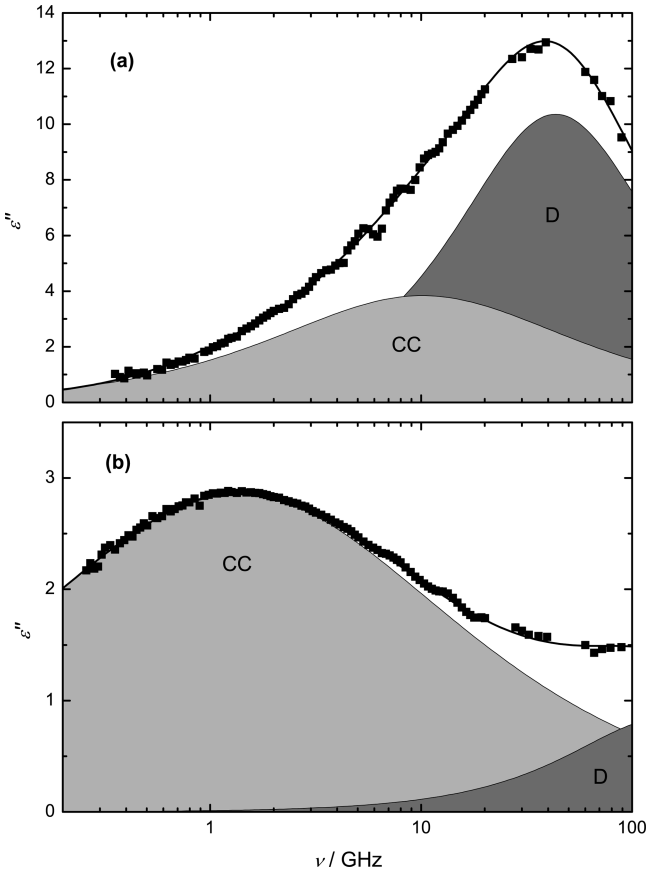

Figure 2. Dielectric loss spectra, $\varepsilon''(\nu)$, of [bmim][BF_4] + AN mixtures at 25 °C at IL mole fractions, x_{IL}, of (a) 0.04389 and (b) 0.7544. Symbols represent experimental data, lines show the CC+D fit, shaded areas indicate the contributions of the individual processes.

4. RESULTS

4.1. Densities and Excess Volumes. Experimental densities obtained by vibrating-tube measurements for [bmim][BF_4] + AN mixtures over the entire composition range at 25 °C are summarized in Table S1 in the Supporting Information.[42] Figure S4 in the Supporting Information compares the observed densities for these mixtures with literature data.[43−47] The present results agree well with the values reported by Zafarani-Moattar and Shekaari[44,47] over the entire composition range, and with those of Wang et al.[43] at $x_{IL} \leq 0.6$, with deviations $|\delta\rho| = |\rho - \rho_{lit}| \leq 2$ kg·m^{-3}. On the other hand, the present densities disagree markedly at all compositions from those reported by two other groups, with $|\delta_\rho| \lesssim 20$ kg·m^{-3},[45,46] and, in the opposite direction, with those of Wang et al.[43] at $x_{IL} > 0.7$, for which $|\delta\rho| \lesssim 10$ kg·m^{-3} (Figure S4). Such differences are, unfortunately, a common occurrence for ILs; they are usually thought to reflect the presence of impurities, especially water or halide ions.[48]

Excess molar volumes, V^E, were calculated from the present densities for [bmim][BF_4] + AN mixtures (Table S1), and from those of ref 29 for the other IL + AN mixtures using the equation

$$V^E = x_{IL}M_{IL}(\rho^{-1} - \rho_{IL}{}^{-1}) + (1 - x_{IL})M_{AN}(\rho^{-1} - \rho_{AN}{}^{-1}) \quad (4)$$

where M_i is the molar mass of component i. The excess volumes so derived are shown in Figure 3, together with the fits obtained using Padé equations[49]

$$V^E/10^{-6}\ \mathrm{m^3\ mol^{-1}} = x_{IL}(1 - x_{IL})\frac{A_1 + A_2(2x_{IL} - 1)}{1 + A_3(2x_{IL} - 1) + A_4(2x_{IL} - 1)^2 + A_5(2x_{IL} - 1)^3} \quad (5)$$

where A_i are adjustable parameters whose magnitudes are listed in Table S5 in the Supporting Information.

The V^E values for all of the present IL + AN mixtures show (Figure 3) marked deviations from ideal mixing ($V^E \equiv 0$). The pronounced asymmetry of the $V^E(x_{IL})$ curves is consistent with the tendency of ILs to maintain their chemical "character" even at relatively high levels of dilution with molecular solvents.[11,12] For each of the present IL + AN mixtures, V^E is negative at all compositions but becomes less negative with increasing cation size: $|V^E([hmim][BF_4])| < |V^E([bmim][BF_4])| < |V^E([emim][BF_4])|$. However, the location of the minimum in V^E, at $x_{IL} \approx 0.27$, is virtually independent of the IL. The negative values of V^E indicate that the binary mixtures pack more efficiently than the neat components, with the highest packing density being achieved at an IL:AN mole ratio of ~1:3.

4.2. General Features of the Dielectric Spectra. Before going on to discuss the DR spectra of the IL + AN mixtures, it is appropriate to consider those of the neat components in

dx.doi.org/10.1021/jp3020673 | J. Phys. Chem. B 2012, 116, 7509–7521

Table 1. Fit Parameters of Eq 3, Assuming a CC+D Model, for the Dielectric Spectra of [emim][BF_4] + AN at 25 °C[a]

x_{IL}	c_{IL}	ε	S_1	τ_1	α_1	S_2	τ_2	ε_∞	$\chi_r^2/10^{-4}$
0	0	35.84				32.51	3.32	3.33	60
0.01082	0.2014	37.31	3.99	60.5	0.31	29.62	3.46	3.69	121
0.01646	0.3036	37.17	5.18	35.0	0.29	28.19	3.49	3.79	182
0.02252	0.4114	37.16	7.03	25[b]	0.29	26.76	3.44	3.38	319
0.04929	0.8621	36.18	11.55	15[b]	0.23	21.06	3.62	3.57	201
0.08059	1.342	34.91	14.91	12.5	0.22	15.47	4.38	4.53	179
0.1218	1.903	32.79	17.15	12.7	0.16	11.41	4.08	4.23	142
0.1736	2.513	30.46	16.98	15[b]	0.13	9.05	4.02	4.42	137
0.2371	3.146	28.15	17.14	17[b]	0.15	6.12	4.95	4.89	130
0.3264	3.867	25.17	16.63	20.4	0.14	3.72	3.53	4.82	57.9
0.4565	4.672	21.97	14.52	27.8	0.16	2.80	2.58	4.65	28.2
0.6520	5.528	18.71	12.03	40.8	0.23	2.34	1.87	4.34	25.4
0.8336	6.092	16.63	10.47	50.5	0.31	1.96	1.66	4.20	6.20
1[c]	6.484	14.5	8.70	46.6	0.36	2.05	1.22	3.75	

[a]Quantities: static permittivities, ε; relaxation times, τ_j; amplitudes, S_j; CC shape parameter, α_1; infinite frequency permittivity, ε_∞, and reduced error function of the overall fit, χ_r^2. Units: c_{IL} in mol·L^{-1}; τ_j in 10^{-12} s. [b]Parameter fixed during fitting procedure. [c]Parameters taken from ref 32.

Table 2. Fit Parameters of Eq 3, Assuming a CC+D Model, for the Dielectric Spectra of [bmim][BF_4] + AN at 25 °C[a]

x_{IL}	c_{IL}	ε	S_1	τ_1	α_1	S_2	τ_2	ε_∞	$\chi_r^2/10^{-4}$
0.003131	0.05883	37.09	3.08	64.7	0.56	31.27	3.25	2.74	133
0.006352	0.1185	37.33	4.01	56.3	0.47	29.69	3.41	3.63	151
0.009414	0.1744	37.69	6.22	31.4	0.52	29.00	3.35	2.47	144
0.01472	0.2696	36.84	6.49	20[b]	0.32	27.40	3.28	2.95	330
0.01981	0.3588	36.79	8.75	15[b]	0.37	25.33	3.41	2.72	231
0.02574	0.4601	36.49	9.42	15[b]	0.27	23.81	3.35	3.26	446
0.03142	0.5545	35.88	8.99	17.4	0.24	23.69	3.44	3.21	245
0.03774	0.6570	35.85	8.76	19.3	0.21	23.18	3.67	3.90	641
0.04389	0.7538	35.53	11.10	15.7	0.23	20.72	3.66	3.71	289
0.05668	0.9472	34.90	12.14	14.9	0.19	18.46	3.84	4.30	595
0.07179	1.162	33.70	12.28	16.7	0.17	17.39	3.97	4.02	186
0.08907	1.392	33.00	13.96	15.5	0.13	14.56	3.88	4.49	618
0.1077	1.622	31.95	14.62	16.5	0.17	12.98	4.33	4.36	167
0.1538	2.123	29.72	14.18	21.5	0.15	10.72	4.82	4.82	123
0.2149	2.666	27.08	13.89	25[b]	0.13	8.17	5.39	5.02	140
0.2966	3.239	24.30	16.08	26.6	0.18	3.50	4.06	4.72	56.1
0.3900	3.741	22.35	17.06	30.9	0.28	1.30	2.03	3.99	36.3
0.6126	4.549	18.07	12.69	71.5	0.34	1.52	1.65	3.86	8.18
0.7544	4.893	16.67	11.72	116	0.42	1.71	1.06	3.24	9.32
0.8943	5.157	15.65	11.08	178	0.50	1.56	0.800	3.01	8.83
1[c]	5.319	14.60	10.03	284	0.52	2.04	0.620	2.57	

[a]Quantities: static permittivities, ε; relaxation times, τ_j; amplitudes, S_j; CC shape parameter, α_1; infinite frequency permittivity, ε_∞, and reduced error function of the overall fit, χ_r^2. Units: c in mol·L^{-1}; τ_j in 10^{-12} s. [b]Parameter fixed during fitting procedure. [c]Parameters taken from ref 32.

some detail, since their features are required for understanding the mixtures.

Acetonitrile. The broadband spectrum of neat AN at 25 °C (Figure 4a) is dominated by a relaxation process centered at ~50 GHz but also exhibits two smaller very-high-frequency modes, centered at ~0.5 and 2 THz,[50,51] outside the range of the present spectra. The inherent broadness of the latter two modes inevitably means that they exert some influence on the AN spectrum in the high GHz region. However, because the ~50 GHz relaxation, which corresponds to the reorientational diffusion of the AN dipoles, dominates $\hat{\varepsilon}(\nu)$ over a very wide range of frequencies, the DR spectrum at $\nu \leq 89$ GHz can be very well fitted with a single Debye equation (the D model, full line in Figure 4a). The static permittivity, ε = 35.84, and relaxation time, τ = 3.32 ps, at 25 °C obtained from this simple model are in quantitative agreement with the corresponding results for the more complex model used to fit the broadband spectrum up to 8 THz.[51] Of course, as would be expected, the value of ε_∞ = 3.33 derived from the D model differs significantly from the far-infrared value of Ohba and Ikawa, ε_∞^{FIR} = 1.814.[50] However, as the D model covers 95% of the total dispersion of AN, restriction of the present spectra to $\nu \leq$ 89 GHz does not significantly affect the analysis of the AN contribution to the DR spectra of the present mixtures.

Ionic Liquids. The dielectric spectra of neat imidazolium ILs[31,41] are somewhat more complicated than that of AN (Figure 4). In addition to a dominant CC relaxation in the 1–10 GHz region, assigned to the highly cooperative jump reorientation of the dipolar cations,[11,32] there is also a low-frequency Debye mode indicative of mesoscopic aggregates.[41] However, in contrast to the corresponding optical Kerr effect spectra,[41] the contribution of this sub-α mode to the dielectric

dx.doi.org/10.1021/jp3020673 | J. Phys. Chem. B 2012, 116, 7509–7521

Table 3. Fit Parameters of Eq 3, Assuming a CC+D Model, for the Dielectric Spectra of [hmim][BF_4] + AN at 25 °C[a]

x_{IL}	c_{IL}	ε	S_1	τ_1	α_1	S_2	τ_2	ε_∞	$\chi_r^2/10^{-4}$
0.004117	0.07700	36.91	2.47	116	0.33	30.81	3.36	3.64	174
0.008445	0.1560	36.98	4.59	39.1	0.37	29.15	3.34	3.24	145
0.01744	0.3142	36.66	5.53	37.6	0.24	27.18	3.59	3.95	221
0.03816	0.6489	35.76	9.55	23.9	0.25	22.06	3.92	4.15	270
0.06486	1.028	34.34	14.84	16.9	0.25	16.28	3.76	3.21	157
0.09763	1.427	32.48	17.35	17.1	0.27	11.57	4.31	3.56	81.9
0.1399	1.855	30.55	19.96	17.1	0.28	6.88	5.08	3.70	88.9
0.1943	2.300	27.78	18.31	25[b]	0.26	5.32	4.98	4.15	76.2
0.2712	2.785	25.28	17.27	35[b]	0.30	3.62	7.23	4.39	80.1
0.3907	3.322	21.40	16.40	46.6	0.33	0.904	3.05	4.10	10.1
0.5902	3.894	17.24	12.46	109	0.40	1.09	1.93	3.69	15.4
0.7435	4.183	14.50	10.06	169	0.45	0.996	1.31	3.45	7.28
0.8889	4.387	12.84	8.72	262	0.52	1.35	0.576	2.77	6.34
1[c]	4.512	12.00	7.87	451	0.54	1.95	0.44	2.18	

[a]Quantities: static permittivities, ε; relaxation times, τ_j; amplitudes, S_j; CC shape parameter, α_1; infinite frequency permittivity, ε_∞, and reduced error function of the overall fit, χ_r^2. Units: c in mol·L^{-1}; τ_j in 10^{-12} s. [b]Parameter fixed during fitting procedure. [c]Parameters taken from ref 32.

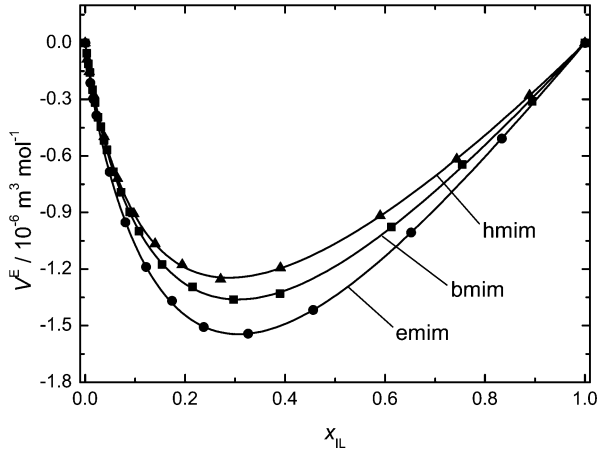

Figure 3. Excess molar volumes, V^E, of binary IL + AN mixtures at 25 °C as a function of the IL mole fraction, x_{IL}: ●, [emim][BF_4]; ■, [bmim][BF_4]; ▲, [hmim][BF_4]. Lines are fits with eq 5,[49] using the parameters listed in Table S5 in the Supporting Information.

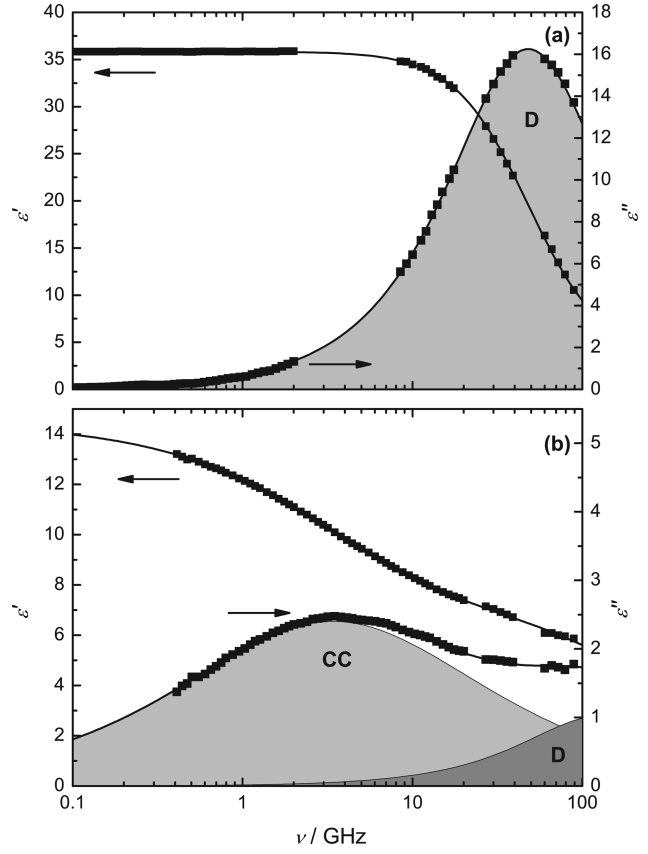

Figure 4. Relative permittivity, $\varepsilon'(\nu)$, and dielectric loss, $\varepsilon''(\nu)$, spectra of (a) neat AN and (b) neat [emim][BF_4] at 25 °C. Full lines are fits with a D model (a) and a CC+D model (b); shaded areas indicate the contributions of the individual processes.

spectrum is very weak so that it can be reasonably subsumed under the low-frequency wing of the dominant CC relaxation.[52] In addition to these low-frequency contributions there are strong resonant features arising from intermolecular vibrations that extend from the terahertz region down to ~50 GHz.[31,41] Fortunately, it has also been demonstrated that for IL spectra restricted to $\nu \leq 89$ GHz the onset of these terahertz modes can be satisfactorily modeled by a Debye equation centered at ~300 GHz without affecting the amplitude(s), relaxation time(s), and band shape(s) of the lower-frequency cation (and, if applicable, anion) mode(s).[11,12,32] Thus, a CC+D model provided a satisfactory empirical description of the spectra for all of the present neat ILs, as shown for example by the full line in Figure 4b.[32] Nevertheless, it has to be kept in mind that for the present mixtures, while the low-frequency CC mode can be quantitatively accounted for on a molecular level, the fast D mode can only be interpreted qualitatively.

IL + AN Mixtures. Figure 1 shows the rather broad and featureless dielectric spectra obtained for representative [bmim][BF_4] + AN mixtures and the neat components. The corresponding spectra for mixtures of AN with [emim][BF_4] or [hmim][BF_4] are given in Figures S2 and S3 in the Supporting Information. The spectra for all the mixtures showed more-or-less smooth variations from that of neat AN to those of the neat ILs (Figure 1, Figures S2 and S3) and could be satisfactorily described by a CC+D model. The variation with composition of the amplitudes, S_j, and relaxation times, τ_j (j = 1, 2), CC width parameter, α_1, and the other dielectric parameters obtained from the spectra, are summarized in Tables 1–3. Because the spectra for all three sets of mixtures, and their variation with composition, are similar the following discussion

dx.doi.org/10.1021/jp3020673 | J. Phys. Chem. B 2012, 116, 7509–7521

will mostly focus on the [bmim][BF_4] + AN mixtures. Essentially identical conclusions can be drawn from the spectra of the other mixtures.

The higher-frequency (D) mode in [bmim][BF_4] + AN mixtures is clearly a composite, analogous to that observed for mixtures of ILs with dichloromethane (DCM),[11,12] since S_2 and τ_2 approach the neat AN values as $x_{IL} \rightarrow 0$ and the neat (faster mode) IL values as $x_{IL} \rightarrow 1$ (Figure 5). Closely similar patterns

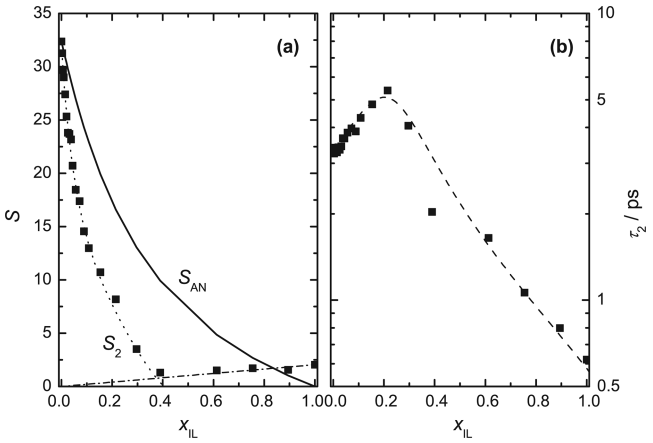

Figure 5. (a) Observed amplitudes, S_2, and (b) relaxation times, τ_2, of the higher-frequency (j = 2) process of [bmim][BF_4] + AN mixtures at 25 °C (filled symbols). In (a) the amplitude S_{AN} (full line) is that predicted using eq 8 for the relaxation of AN molecules at c_{AN}; the IL contribution to S_2 (dash-dotted line) was assumed to increase linearly with x_{IL}; and the dotted line is S_2 reduced by the IL contribution. In (b) the dashed line is only a visual guide.

of behavior were observed for the other sets of mixtures (Figure S5, Supporting Information). For all mixtures at low x_{IL}, S_2 decreased steeply from the neat AN value (~32.5) to $S_2 \approx 1$ at $x_{IL} \approx 0.4$, which suggests that at $x_{IL} \lesssim 0.4$ this relaxation process largely reflects the bulk AN mode (Figure 5a, and Figure S5a,c). At $x_{IL} \gtrsim 0.4$, S_2 essentially reflects the contributions expected from the IL concentration. In contrast to the amplitude, τ_2 passed through a well-defined maximum at $x_{IL} \approx 0.2$ for all systems (Figures 5b, and Figure S5b,d).

For all ILs investigated previously, the CC modes observed at low frequencies could be ascribed to the cooperative reorientation of the cations[12,32,41] and it is reasonable to assume that cation reorientation is also an important contribution to the low-frequency mode of the present mixtures. On addition of AN to the neat ILs, τ_1 and α_1 decrease gradually, reaching a minimum at $x_{IL} \approx 0.1$, before rising sharply as $x_{IL} \rightarrow 0$ (Figure 6, and Figure S6 in the Supporting Information). Similar behavior was observed for IL + DCM mixtures at low x_{IL} and was attributed to the formation of ion pairs.[11,12] As discussed below, ion pairing is also important in the present solutions. However, in contrast to IL + DCM mixtures, the values of S_1 for IL + AN (Figure 7, and Figure S7 in the Supporting Information) exhibit a pronounced maximum at $x_{IL} \approx 0.25$ before sharply dropping to zero as $x_{IL} \rightarrow 0$. This feature is thought to be due to a significant contribution from AN dipoles coupled to (solvating) the imidazolium cations (see below).

5. DISCUSSION

5.1. Higher-Frequency Mode. *Relaxation times.* The dielectric relaxation of neat AN centered at ~50 GHz is due to

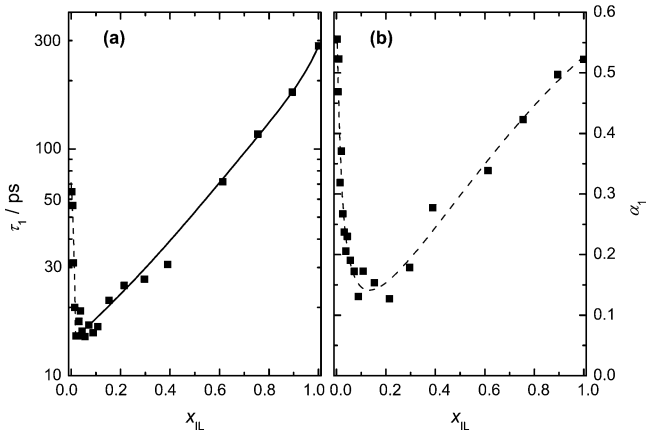

Figure 6. (a) Average relaxation time, τ_1, and (b) Cole–Cole broadness parameter, α_1, of the lower-frequency (j = 1) process of the CC+D model for [bmim][BF_4] + AN mixtures at 25 °C. Solid line in (a) is calculated from a fit of $\tau_1' = f(\eta)$ with eq 7, see text; dashed lines are only visual guides.

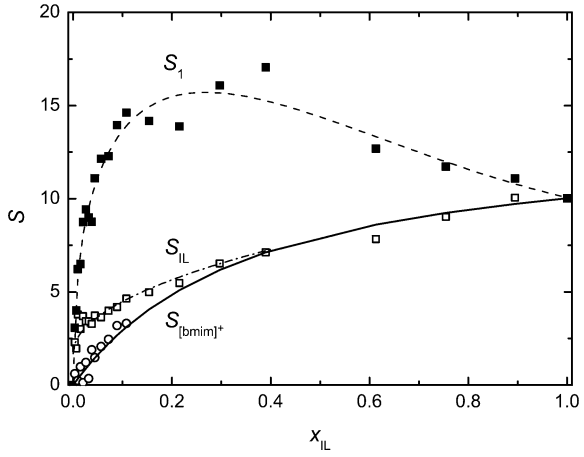

Figure 7. Experimental amplitude of relaxation process 1, S_1 (■, dashed line is a visual guide), obtained assuming the CC+D model, and the corresponding IL contribution, S_{IL} (□, dash-dotted line is a visual guide) calculated from eq 10b, for [bmim][BF_4] + AN mixtures at 25 °C. The full line indicates the cation relaxation amplitude, $S_{[bmim]^+}$, predicted from the analytical IL concentration via eq 8. The open circles (○) show the corresponding data derived from the parameters of the D+CC+D model at $x_{IL} \leq 0.1077$.

the rotational diffusion of its molecular dipoles.[53] The molecular rotational correlation time, τ', can therefore be obtained from the observed (macroscopic) dielectric relaxation time, τ, and width, α, of the associated dispersion step through the Powles–Glarum equation[54]

$$\tau' = \tau\left(\frac{2\varepsilon + \varepsilon_\infty}{3\varepsilon}\right)^{1/(1-\alpha)} \quad (6)$$

Note that for a Debye process $\alpha = 0$ and eq 6 reduces to its more usual form for such processes.[55]

The molecular rotational correlation time can be linked to the bulk dynamic viscosity, η, through the Stokes–Einstein–Debye (SED) equation[56]

$$\tau' = \frac{3V_{eff}\eta}{k_B T} + \tau^0 \quad (7)$$

dx.doi.org/10.1021/jp3020673 | J. Phys. Chem. B 2012, 116, 7509–7521

where V_{eff} is the effective volume of rotation of the relaxing species, k_B the Boltzmann constant, T the thermodynamic temperature (in Kelvin), and τ^0 the empirical axis intercept, which is sometimes interpreted as the free-rotator correlation time.[56] The effective volume, $V_{eff} = V_m f_\perp C$, is determined by the molecular volume of the rotating dipole, V_m, a geometric factor, $f_\perp$, accounting for its deviation from spherical shape,[57] and the hydrodynamic coupling parameter, C, connecting macroscopic to local viscosity. Experimental coupling parameters obtained with eq 7 are generally between the theoretical limits for stick, $C_{stick} = 1$, and slip, $C_{slip} = 1 - f_\perp^{-2/3}$, boundary conditions.

As noted in section 4, the variation of S_2 and τ_2 with x_{IL} (Figures 5, and Figure S5 in the Supporting Information) suggests that the higher-frequency mode is dominated by the reorientation of AN molecules at $x_{IL} \lesssim 0.4$. Given that τ_2 exhibits a pronounced maximum at $x_{IL} \approx 0.2$ (Figure 5b), while η increases monotonically with x_{IL},[43] it is not surprising that the SED model, eq 7, breaks down at moderate IL content. In contrast, at $x_{IL} \leq 0.16$ a good linear correlation is found between τ_2' and η (Figure 8). This observation, together with

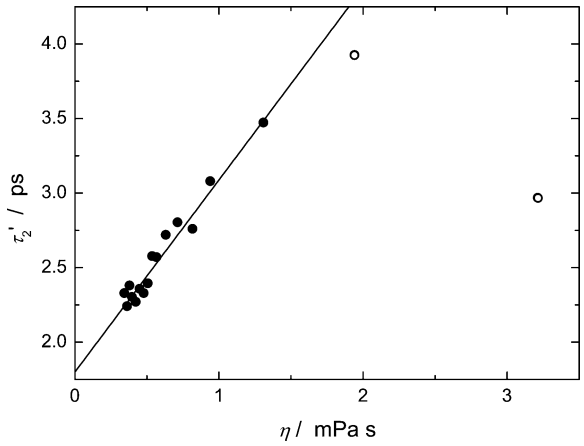

Figure 8. Molecular rotational correlation times of process 2, τ_2' (symbols), in the CC+D model for [bmim][BF_4] + AN mixtures at 25 °C as a function of bulk solution viscosity, η,[43] at $0 \leq x_{IL} \leq 0.1539$. Full line represents eq 7; hollow symbols correspond to x_{IL} values where eq 7 is no longer applicable (see text).

the fact that the high-frequency mode in AN-rich mixtures is well described by a Debye equation, indicates that for $x_{IL} \lesssim 0.16$ the AN molecules experience an essentially homogeneous environment with local fluctuations rapidly averaged out.

From the slope of $\tau_2'(\eta)$ at $x_{IL} \leq 0.16$ (Figure 8) a value of $C = 0.033$ was obtained assuming the neat AN values[66] of $V_m = 43.9$ Å^3 and $f_\perp = 1.208$. This value of C is approximately half of those found by Barthel et al.[53] for AN solutions of Bu_4NBr ($C = 0.068$) and NaI ($C = 0.063$), both of which are considerably smaller than the theoretical limiting value for slip boundary conditions, $C_{slip} = 0.118$.

Similar discrepancies arising from the slope of eq 7 (and the C parameter derived from it), when viscosity was varied either by changing the concentration of a salt or by changing the temperature of the neat solvent, have also been observed for electrolyte solutions in dimethylformamide and dimethylacetamide.[58] Collectively, these data suggest that the increase of η in salt solutions is essentially due to the mixing of different-sized particles (solvent molecules and solvated ions). Furthermore, they imply that ion−solvent interactions are essentially restricted to the first solvation shell of the ions, such that the frictional forces acting on the bulk solvent molecules increase only weakly with electrolyte concentration.[58] Given that the present spectra indicate that for $x_{IL} \lesssim 0.2$ these mixtures behave like conventional electrolyte solutions, values of $C \approx 0.06$ might be expected. Since the observed values are even lower ($C \approx 0.03$), this suggests either that the IL cation and anion are especially poorly solvated by AN or possibly that partial demixing (microheterogeneity), as suggested by computer simulations,[6,8,9] may be occurring. Further investigation would be required to resolve these issues.

Amplitudes. The observed amplitude of a dielectric relaxation process can be analyzed in terms of the Cavell equation

$$\frac{2\varepsilon + 1}{\varepsilon} S_j = \frac{N_A}{k_B T \varepsilon_0} c_j \mu_{eff,j}^2 \tag{8}$$

which relates the amplitude S_j of process j to the molar concentration c_j and effective dipole moment $\mu_{eff,j}$ of the species responsible for that process.[59] In condensed phases the reaction field of the surrounding medium polarizes the rotating dipoles, enhancing their gas-phase moment μ_j. This produces an apparent moment, $\mu_{ap,j} = \mu_j/(1 - f_j\alpha_j)$, where f_j is the reaction field factor and α_j is the polarizability of the dipole. Additionally, the relative orientations of the dipoles may be correlated, which is taken into account by an empirical correlation factor, g_j, with $\mu_{eff,j} = \mu_{ap,j}(g_j)^{1/2}$.[60]

Figure 5a, and Figure S5a,c in the Supporting Information, compare the experimental S_2 values of the IL + AN mixtures (symbols) with the amplitudes S_{AN} calculated for AN molecules via eq 8 on the basis of their analytical concentration, c_{AN} (full line). This assumes that AN molecules in the mixtures have the same effective dipole moment as in neat AN, $\mu_{eff,AN} = 4.34$ D, calculated via eq 8 using $\varepsilon = 35.84$ (Table 1) and $\varepsilon_\infty = 1.814$.[50] Two features of Figure 5a and Figure S5a,c are noteworthy. First, at low x_{IL}, the experimental amplitudes are well below the contribution expected from c_{AN}, i.e., $S_2 \ll S_{AN}$, with the difference increasing with increasing IL content at $x_{IL} \lesssim 0.4$. In other words, the observed S_2 values are increasingly lower than what would be expected from the analytical amount of AN in the mixtures. Thus, at $x_{IL} \gtrsim 0.4$ (possibly a little higher for [emim][BF_4], see Figure S5a), there are in essence no "free" AN molecules ($S_2 \to 0$). Second, and consistent with this deduction to a good approximation, the S_2 values at $x_{IL} \gtrsim 0.4$ lie on the straight (dash-dotted) line connecting the origin ($x_{IL} = 0$, $S_2 = 0$) with the amplitude of the fast mode of the neat IL. Thus, at $x_{IL} \gtrsim 0.4$ the amplitude of the high-frequency mode of the mixtures mainly reflects the librations and intermolecular vibrations of the IL component.

The apparent (i.e., DR-detectable) concentration of AN in the mixtures, c_{AN}^{ap}, was calculated via eq 8 from the observed S_2 values corrected for the contribution from the IL component. The fraction of AN molecules contributing to S_2, c_{AN}^{ap}/c_{AN}, does not decrease monotonically but instead shows a break at $x_{IL} \approx 0.2$ (Figure 9, and Figure S8 in the Supporting Information), coinciding with the maximum in τ_2 (Figure 5, b and d). This break in Figure 9 and Figure S8 may suggest that there are two processes that remove essentially "free" AN molecules in the mixtures at $x_{IL} < 0.4$. The first process, which dominates at $x_{IL} \lesssim 0.2$, is almost certainly associated with the solvation (binding) of the $[Rmim]^+$ cations by the AN molecules. In mixtures where AN is predominant, it is convenient to express

dx.doi.org/10.1021/jp3020673 | J. Phys. Chem. B 2012, 116, 7509−7521

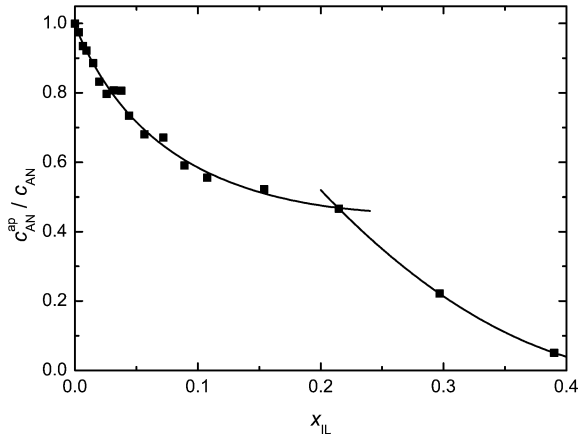

Figure 9. Fraction of AN molecules, c_{AN}^{ap}/c_{AN} (symbols), contributing to the amplitude S_2 of [bmim][BF_4] + AN mixtures at 25 °C as a function of the IL mole fraction, x_{IL}; lines are a visual guide only.

the amount of "solvent" (AN) so bound in terms of an effective solvation number per "solute" (IL) particle

$$Z = (c_{AN} - c_{AN}^{ap})/c_{IL} \quad (9)$$

In these calculations it was assumed that the effective dipole moment of AN in the mixtures was the same as in neat AN. The results (Figure 10) show that at a given composition Z is

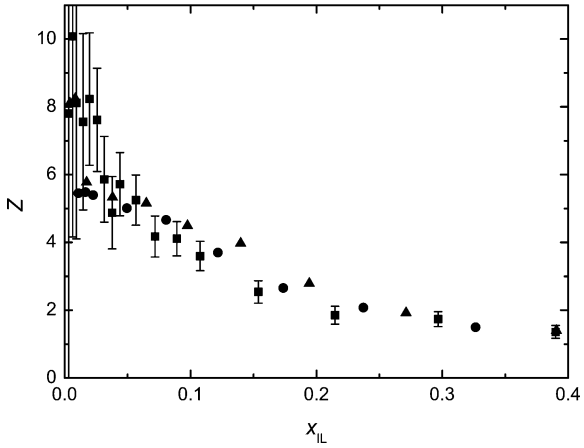

Figure 10. Effective solvation numbers, Z, of ILs by AN in binary IL + AN mixtures at 25 °C as a function of the IL mole fraction, x_{IL}: ●, [emim][BF_4]; ■, [bmim][BF_4]; ▲, [hmim][BF_4]. Representative error bars correspond to an uncertainty of ±1.2 in S_2.[62]

virtually the same for all three imidazolium salts, irrespective of the length of their *n*-alkyl chain. This strongly implies that these bound AN molecules are mainly interacting with the polar headgroup (imidazolium ring) of the cation rather than the alkyl chain. The general decrease in Z with increasing x_{IL}, albeit with a possible "break" at $x_{IL} \approx 0.2$ (Figure 10), is typical of the behavior of conventional electrolyte solutions and is usually explained by solvation-shell overlap.[22]

At $x_{IL} \gtrsim 0.2$ a second process occurs which further removes "free" AN, causing another drop in c_{AN}^{ap}/c_{AN} (Figure 9, and Figure S8 in the Supporting Information) to approximately zero. This second process might reflect either solvation of the (now more concentrated) anions by the AN (even though anion solvation in AN is known to be weak[61]) or possibly to cluster (microphase) formation. However, no specific information about such effects is provided by the present spectra.

5.2. Lower-Frequency Mode. As indicated above (section 4.2), both the relaxation time, τ_1, and the associated width parameter, α_1, of the lower-frequency CC mode in [bmim][BF_4] + AN mixtures exhibit pronounced minima at $x_{IL} \approx 0.06$ and ~0.16, respectively (Figure 6). Similar minima were found for the other two sets of mixtures (Figure S6 in the Supporting Information). All of the mixtures also show a weak but clearly detectable maximum in their static permittivities, ε (Figure S9 inset, Supporting Information). Similar features were recently observed for DCM mixtures with [bmim][BF_4][11] and [emim][$C_2H_5SO_4$][12] and were unequivocally assigned to the presence of contact ion pairs (CIPs) at low x_{IL}, with the minimum in τ_1 roughly marking a smooth transition from electrolyte-solution-like to molten-salt-like character.

For neat imidazolium ILs there is good evidence[32,41,63,64] that the low-frequency CC relaxation (the "α relaxation" of ref 41) is associated with cation reorientation occurring through large-angle jumps, triggered by slow cage fluctuations associated with a sub-α relaxation that dominates time-resolved optical Kerr effect (OKE) spectra at low frequencies.[41] This jump reorientation of the cations is highly cooperative, involving concerted rotational and translational motions of the surrounding ions. The spread of environments ("cages") experienced by the cations, which is probed by the width parameter α_1, is rather wide.[12,63,64] The available data for IL + DCM mixtures[11,12] indicate that this jump-relaxation mechanism prevails down to $x_{IL} \approx 0.3$, with the added molecular liquid (DCM) acting as a "lubricant", shortening the lifetimes and reducing the heterogeneity of the "cages". The smooth decrease of τ_1 and α_1 on dilution of the stock ILs with AN (Figure 6, and Figure S6 in the Supporting Information) suggests that this is also the case for the present mixtures, now even down to $x_{IL} \approx 0.2$. This picture is further supported by the viscosity dependence of τ_1 for [bmim][BF_4] + AN. Over the composition range $0.21 \leq x_{IL} \leq 1$ the molecular correlation times obtained with eq 6 seem to follow the SED model, eq 7. However, as in previous studies of ILs,[12,32,65] the derived volume of rotation, $V_{eff,1}$ = 1.6 Å^3 (≈0.002V_m!), is far too small to be compatible with the rotational diffusion of the cations.

While sharing the same trends with composition, there are IL-specific differences in τ_1 and α_1. At a given x_{IL}, τ_1 values are always in the order [emim][BF_4] < [bmim][BF_4] < [hmim][BF_4], indicating that cation size (MOPAC[66] values for V_m are [emim]$^+$, 510 Å^3; [bmim]$^+$, 750 Å^3; [hmim]$^+$, 1230 Å^3) is, as would be expected, relevant for their jump reorientation. The width parameter, α_1, shows the same sequence as for τ_1 at intermediate x_{IL} but varies in the order [emim][BF_4] ≈ [bmim][BF_4] < [hmim][BF_4] at the minimum in α_1 ($x_{IL} \approx 0.2$), and in the order [emim][BF_4] < [bmim][BF_4] ≈ [hmim][BF_4] for the neat ILs. That is, at an IL:AN mole ratio of ~1:4, [emim]$^+$ and [bmim]$^+$ experience a similar rather narrow ($\alpha_1 \approx 0.15$) spread of environments, whereas for [hmim]$^+$ the dynamical (and presumably structural) heterogeneity is significantly larger ($\alpha_1 \approx 0.25$). This may be related to the greater flexibility of the *n*-hexyl side chain. For the neat ILs the width parameters of [bmim]$^+$ and [hmim]$^+$ are quite large and essentially equal ($\alpha_1 \approx 0.54$) whereas for [emim]$^+$, with its smaller number of conformers, $\alpha_1 \approx 0.35$. This difference may be indicative of the microphase separation suggested by computer simulations of neat ILs.[67]

dx.doi.org/10.1021/jp3020673 | J. Phys. Chem. B 2012, 116, 7509–7521

Figure 7 compares for [bmim][BF_4] + AN mixtures the observed amplitude of process 1, S_1 (filled symbols), with $S_{[bmim]^+}$ (full line). The latter is estimated via eq 8 assuming that all cations present contribute to the low-frequency CC mode and that their dipole moment is the same as in the neat IL, $\mu_{eff,+} = \mu_{eff,IL} = 4.4$ D.[32] Similar plots for [emim][BF_4] or [hmim][BF_4] + AN mixtures are shown in Figure S7 in the Supporting Information. In all cases the experimental values of S_1 cannot be accounted for the presence of the dipolar IL cations alone. Although an ion-pair contribution is expected at low IL mole fractions, say $x_{IL} \lesssim 0.2$, it is unlikely that such a species can account for the large differences between S_1 and $S_{[bmim]^+}$ at $x_{IL} \gtrsim 0.2$.

The analysis of S_2 (section 5.1) revealed that a significant fraction of the AN dipoles in IL + AN mixtures is "bound" (Figure 9, and Figure S8 in the Supporting Information). However, the low surface-charge density of the imidazolium cations,[68] the modest donor (cation solvating) properties of AN,[69] and its very weak acceptor (anion solvating) abilities[53,61] make it unlikely that such AN molecules are actually "frozen" (irrotationally bound)[22] on the DR time scale. Since a separate relaxation mode for these AN molecules is not observed, it appears that, rather than being irrotationally bound, the dynamics of these molecules must be slowed down only to the extent that they (coincidentally) overlap the IL relaxation. Therefore, the observed amplitude of the CC mode, S_1, is the sum of contributions from the IL, S_{IL}, and the "slow" AN, S^S_{AN}

$$S_1 = S_{IL} + S^S_{AN} \tag{10a}$$

Since S^S_{AN} can be estimated (see section 5.1) from process 2 as $S^S_{AN} = (S_{AN} - S_2)$ the empirical IL contribution to the CC amplitude can be calculated as

$$S_{IL} = S_1 - (S_{AN} - S_2) \tag{10b}$$

When doing so it is assumed that the relaxation of "free" AN dominates S_2 at $x_{IL} \leq 0.4$ but is negligible at higher IL content (as shown in Figure 5a,c).

Thus, the values of S_1 (Figure 7, filled squares) are considerably larger than those calculated for the IL, S_{IL}, from the CC+D model (Figure 7, hollow squares). As just argued, this difference is ascribed to the presence of "slow" AN molecules, solvating the IL. It is noteworthy that S_{IL} is essentially identical with the expected cation contribution, $S_{[bmim]^+}$ (full line), at $x_{IL} \gtrsim 0.4$. This indicates that, for the low-frequency CC mode at $x_{IL} \gtrsim 0.4$, the relaxation of $[bmim]^+$ occurs in environments similar to those in the neat IL (thus having the same $\mu_{eff,+} = 4.4$ D[32]). However, at $x_{IL} \lesssim 0.2$, the empirical IL amplitude, S_{IL}, is significantly larger than the expected cation contribution, $S_{[bmim]^+}$, which suggests the presence of an additional dipolar species, with a dipole moment significantly larger than that of $[bmim]^+$. This conclusion is supported by the variation with composition of the effective dipole moment of the IL component, $\mu_{eff,IL}$, calculated with eq 8 from S_{IL} using the analytical IL concentration, c_{IL}. As [bmim][BF_4] is diluted with AN (Figure 11), $\mu_{eff,IL}$ remains constant ($\approx\mu_{eff,+} = 4.4$ D) down to $x_{IL} \approx 0.2$ before rising sharply to 21.1 D as $x_{IL} \to 0$. A similar picture (Figure S10, Supporting Information) is obtained for [emim][BF_4] ($\mu_{eff,IL} \approx \mu_{eff,+} = 3.8$ D at $x_{IL} \gtrsim 0.2$; $\lim_{x_{IL}\to 0}\mu_{eff,IL} = 11.1$ D) and [hmim][BF_4] ($\mu_{eff,IL} \approx \mu_{eff,+} = 4.6$ D at $x_{IL} \gtrsim 0.3$; $\lim_{x_{IL}\to 0}\mu_{eff,IL} = 15.9$ D).

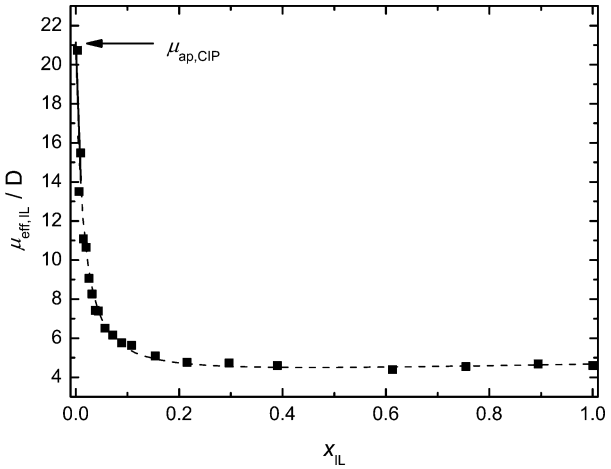

Figure 11. Effective dipole moments, $\mu_{eff,IL}$, of the IL species contributing to S_1 in [bmim][BF_4] + AN mixtures at 25 °C as a function of the IL mole fraction, x_{IL}. The extrapolated value of the apparent dipole moment for the ion pair, $\mu_{ap,CIP}$, is indicated by the arrow.

Plots of $\mu_{eff,IL}$ against x_{IL} (Figure 11, and Figure S10 in the Supporting Information) suggest a transition from IL-like to electrolyte-solution-like behavior at $x_{IL} \approx 0.2$ for all three sets of mixtures. Similar to IL + DCM mixtures,[11,12] the maximum in the static permittivity ε (Figure S9 inset), as well as the strong increase of $\mu_{eff,IL}$ (Figure 11 and Figure S10), and of τ_1 and α_1 (Figures 6 and Figure S6) as $x_{IL} \to 0$ are collectively indicative of ion pair formation at low IL concentrations. A further indication of significant ion pairing in the present mixtures comes from the fact that at $x_{IL} \lesssim 0.15$ the DR spectra can be equally well fit by a D+CC+D model (Tables S2–S4 in the Supporting Information) as by the CC+D model used at higher x_{IL}. The relaxation time and amplitude of the fastest (Debye) mode of this D+CC+D model agree well with those of the high-frequency (D) process of the CC+D model. In other words, the CC mode splits into a lower-frequency D and a higher-frequency CC relaxation. The latter (CC) mode has τ_1, α_1, and S_1 (Tables S2–S4) that vary smoothly from values of the corresponding (CC) mode of the CC+D model at higher x_{IL} (Tables 1–3). The additional D mode emerging at ~1 GHz as x_{IL} decreases below ~0.2 has an amplitude, S_{CIP}, and relaxation time, τ_{CIP}, that are compatible with an ion-pair relaxation.[22] Consistent with the low charge densities of the ions involved and the relatively weak ion solvation in the present systems (see above), it is reasonable to assume that only contact ion pairs (CIPs) of 1:1 stoichiometry are formed. This is corroborated by comparison of the values of V_{eff} (342, 841, and 442 Å^3 for [emim][BF_4], [bmim][BF_4], and [hmim][BF_4], respectively), calculated from τ_1' via eqs 6 and 7, with the corresponding molecular volumes, V_m, of the 1:1 CIPs (570, 964, and 1348 Å^3) calculated using MOPAC.[66] Further support for CIP formation comes from a recent MD simulation study[70] which also concludes that AN addition to [bmim][BF_4] enforces CIP stability and that this effect was most pronounced at the lowest IL content studied, $x_{IL} = 0.1$.[70] Also, using high-pressure infrared spectroscopy, Umebayashi et al.[27] found convincing evidence for CIPs in dilute solutions of the ILs [emim][TFSA] and [emim][FSA] in AN.

Ion Pairing. Application of eq 8 to an equilibrium of 1:1 CIPs and free ions in a dilute solution of an IL in AN gives

dx.doi.org/10.1021/jp3020673 | J. Phys. Chem. B 2012, 116, 7509–7521

$$S_{IL} = \frac{\varepsilon}{2\varepsilon + 1}\frac{N_A}{k_B T \varepsilon_0}\{(c_{IL} - c_{CIP})\mu_{eff,+}^2 + c_{CIP}\mu_{eff,CIP}^2\} \quad (11)$$

where $c_{IL} = c_+ + c_{CIP}$ is the total concentration of the IL, and c_+ and c_{CIP} are respectively the concentrations of free cations and CIPs. It is further assumed that the solution is dilute enough to neglect orientational correlations between the cations and ion-pair dipoles, so that $\mu_{eff,+} = \mu_{ap,+}$ and $\mu_{eff,CIP} = \mu_{ap,CIP}$ over the concentration range of interest. Values of c_{CIP} can then be obtained from eqs 10b and 11 using S_1, provided reasonable values for $\mu_{ap,+}$ and $\mu_{ap,CIP}$ are known.

The values of $\mu_{eff,+}$, calculated for the present cations in the neat ILs ([emim]$^+$, 3.8 ± 0.3 D; [bmim]$^+$, 4.4 ± 0.9 D; [hmim]$^+$, 4.6 ± 1.8 D)[32] are in reasonable agreement with quantum-chemical calculations of $\mu_{ap,+}$ = 4.9 ± 0.7 D for [bmim]$^+$ embedded in a dielectric continuum with the permittivity of neat [bmim][BF$_4$].[71] Furthermore, $\mu_{eff,+}$ remains constant for the present ILs at $0.5 \lesssim x_{IL} \leq 1$, where individual long-lived ion pairs are unlikely (Figure 11). Thus, it may reasonably be assumed that $\mu_{ap,+} = \mu_{eff,+}(x_{IL}=1)$.

The value of $\mu_{eff,IL}$ increases strongly with dilution (Figure 11, and Figure S10 in the Supporting Information). To a first approximation, its limiting value at $x_{IL} \to 0$ can be assigned to the apparent dipole moment of the relevant CIP: $\mu_{eff,CIP}$ = 11.1 D for [emim][BF$_4$], 21.1 D for [bmim][BF$_4$], and 15.9 D for [hmim][BF$_4$]. For comparison, a value of $\mu_{eff,CIP}$ = 22.0 D was obtained using the same approach for the CIP of [bmim][BF$_4$] in DCM.[11] These results are also broadly consistent with the apparent dipole moments calculated using MOPAC[66] for CIPs in a dielectric continuum with $\varepsilon = \varepsilon_{AN}$. Depending on the conformer, these calculations yield values of ~17.7−19.8 D for [emim][BF$_4$], ~18.6−23.1 D for [bmim][BF$_4$], and ~18.4−26.3 D for [hmim][BF$_4$].

The results obtained for c_{CIP} using the "experimental" values of μ_{eff} (Figure 11 and Figure S10) are plotted in Figure 12, together with the association constants, $K_A = c_{CIP}/(c_{IL} - c_{CIP})^2$ derived from them. The latter can be used to estimate the corresponding standard state (infinite dilution) association constant, K_A°, by extrapolation with (for convenience) a Guggenheim-type equation[24]

$$\log K_A = \log K_A^\circ - \frac{2A_{DH}\sqrt{I}}{1 + R_{ij}B_{DH}\sqrt{I}} + A_K I + B_K I^{3/2} \quad (12)$$

where I ($\equiv c_{IL}$) is the stoichiometric ionic strength; A_{DH} = 1.643 L$^{1/2}$ mol$^{-1/2}$ and B_{DH} = 4.857 × 10^9 L$^{1/2}$ mol$^{-1/2}$ are the Debye−Hückel constants for activity coefficients in AN at 25 °C,[72] R_{ij} = 0.945 nm is the upper limit of ion association,[73] and Y_K ($Y = A, B$) are adjustable parameters. The values of log K_A° follow the order [emim][BF$_4$] > [bmim][BF$_4$] > [hmim][BF$_4$] (Table 4), consistent with the decreasing charge density of the cations and similar to the pattern observed for IL solutions in DCM.[74]

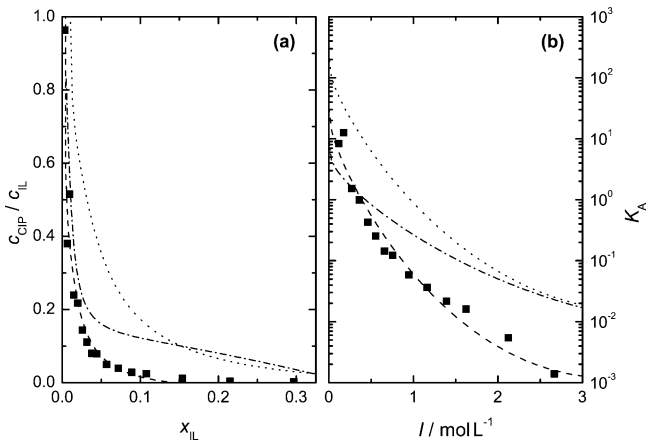

Figure 12. (a) Relative contact ion pair concentrations, c_{CIP}/c_{IL} and (b) association constants, K_A, of [emim][BF$_4$] (dotted line), [bmim][BF$_4$] (dashed line), and [hmim][BF$_4$] (dash-dotted line) in IL + AN mixtures at 25 °C. For visual clarity, experimental data are included only for [bmim][BF$_4$]. Lines in (b) represent fits with eq 12. Note that $c_{CIP}/c_{IL} \to 0$ as $x_{IL} \to 0$.

Table 4. Present and Literature Values of the Standard Association Constants, log K_A°, and Parameters Y_K of Eq 12 for [Rmim][BF$_4$] (R = e, b, h) in AN solution at 25 °C[a]

	CC+D[b]			D+CC+D[b]			lit.[c]
IL	log K_A°	A_K	B_K	log K_A°	A_K	B_K	log K_A°
[emim][BF$_4$]	2.39	−2.96	1.02	2.30	−3.59	1.32	1.20
[emim][BF$_4$][d]	1.15	−2.01	0.64				
[bmim][BF$_4$]	1.53	−3.53	1.29	1.71	−6.04	3.25	1.06
[bmim][BF$_4$][d]	1.06	−3.14	1.11				
[hmim][BF$_4$]	0.99	−1.50	0.436	1.30	−2.61	1.02	1.22

[a]Units: K_A° in L·mol^{-1}; A_K in L·mol^{-1}; B_K in L$^{3/2}$·mol$^{-3/2}$. [b]Present work, see text. [c]Reference 75, using conductivity measurements. [d]$\mu_{ap,IP}$ increased arbitrarily as described in the text.

An alternative way to obtain the ion-pair amplitudes is to fit the spectra at $x_{IL} < 0.2$ with the D+CC+D model (section 3 and Tables S2−S4 in the Supporting Information), since the low-frequency Debye relaxation of this model is ascribed to the reorientation of CIPs. Combining the amplitudes S_{CIP} so obtained (Tables S2−S4) and $\mu_{eff,CIP}$ (see above) calculated with eq 8 yields c_{CIP}. However, it must be kept in mind that the proximity of this small-amplitude D mode to the dominant CC mode *and* to the lower-frequency limit of the measurements makes a reliable estimation problematic. This is due respectively to parameter coupling and the increasing error in the conductivity correction as $\nu \to \nu_{min}$ (eq 2). In consequence, the values of S_{CIP} obtained in this way scatter considerably for the present spectra, where $S_{CIP}/(\varepsilon - \varepsilon_\infty) \lesssim 0.08$. In spite of these difficulties, the log K_A° values obtained from the above analysis of the CC+D model are in good agreement with those derived directly as just described from the D+CC+D model (Table 4). Additionally, the cation amplitudes, $S_{[bmim]^+}$, calculated from c_{CIP} and c_+ on the basis of the D+CC+D model at $x_{IL} \lesssim 0.1$ (hollow circles in Figure 7 and Figure S7) agree well with the cation contribution predicted by the analytical IL concentration (full line in Figure 7 and Figure S7).

While the above agreement in the K_A° values derived from the two models is gratifying, it must be noted that for [bmim][BF$_4$] and especially for [emim][BF$_4$] the K_A° values obtained from DRS using either the CC+D or the D+CC+D models are considerably larger than those determined from conductivity

dx.doi.org/10.1021/jp3020673 | J. Phys. Chem. B 2012, 116, 7509−7521

measurements[73] (Table 4). This is almost certainly a reflection of the experimental and theoretical uncertainties involved in the DRS measurements. In particular, because the fraction of free ions is relatively high in the AN-rich solutions, the extrapolation of $\mu_{eff,+}$ to $x_{IL} = 0$ will underestimate the ion-pair dipole moment, in contrast with the much more highly associated ILs, in DCM.[11,12] To illustrate this point, an arbitrary increase of 50% in the "experimental" value of $\mu_{ap,CIP} = 11.1$ D for [emim][BF_4] gives a K_A° value in good agreement[76] with the conductometric result (Table 4). For [bmim][BF_4] an increase of $\mu_{ap,CIP} = 21.1$ D by 30% is sufficient. While it is emphasized that these adjustments are purely arbitrary, the values of $\mu_{ap,CIP}$ so produced are still reasonable, keeping in mind the uncertainties in the ion-pair dipole moments calculated with MOPAC (see above). For [hmim][BF_4] the conductometric K_A° lies between the values obtained from the CC+D and the D +CC+D models so adjustments are not appropriate.

Despite the uncertainties, the present spectra provided useful information on ion pairing and ion solvation of the investigated ILs (Table 4) in AN. Because of the numerous assumptions involved and the lengthy extrapolation to $I = 0$, the present DRS results for K_A° are almost certainly less reliable than those obtained from high-precision conductivity measurements.[75,76] Nevertheless, they confirm that ion association of [Rmim]-[BF_4] in AN is rather weak and that it is broadly comparable with that of simple 1:1 electrolytes,[53,77,78] like $NaBPh_4$ (log K_A° = 1.14), $LiClO_4$ (1.34), Bu_4NClO_4 (1.40), Bu_4NBPh_4 (1.46), or LiBr (2.17) in this solvent. The present data also indicate that the value of log $K_A^\circ = 2.85$ reported by Wang et al.[79] for [bmim][BF_4] in AN, using low-precision conductivity data, is almost certainly too high.

It is noteworthy that for $x_{IL} > 0.05$ the relative ion-pair concentrations, c_{CIP}/c (Figure 12a), and the corresponding $K_A(I)$ values (Figure 12b), of [hmim][BF_4] are considerably larger than the corresponding values for the other ILs. This is consistent with the greater abundance of microdomains in mixtures of imidazolium ILs with AN with increasing alkyl side-chain length of the cation, seen in MD simulations.[67]

6. CONCLUDING REMARKS

The present dielectric spectra for binary mixtures of ILs with AN at 25 °C, in the frequency range $0.2 \lesssim \nu/\text{GHz} \leq 89$, can be satisfactorily fitted over the entire composition range by assuming just two relaxation modes: a Cole−Cole process at lower frequencies and a faster Debye process. Detailed analysis of these two modes has shown that both are superpositions of more than one process.

The slower CC process, centered at ~2 GHz, is associated with the reorientation of the dipolar imidazolium cations, but is overlapped by a contribution from "slow" AN molecules solvating those cations and, at $x_{IL} \lesssim 0.2$, a contribution from contact ion pairs. The faster Debye mode centered at ~50 GHz is due to the rotational diffusion of essentially free AN molecules combined with the low-frequency wing of the very fast (THz) intermolecular vibrations and librations of the ILs.

As found previously for IL + DCM mixtures,[11,12] the ILs retain their chemical character up to high dilution with AN ($x_{IL} \gtrsim 0.2$). At $x_{IL} \lesssim 0.2$ the ILs behave like conventional, rather weakly associated electrolytes in AN. Consistent with the relatively weak solvation of both ions by AN, only CIPs appear to be formed, becoming dominant at $x_{IL} \lesssim 0.05$.

In essence, IL + AN mixtures can be divided into two regions. At low IL concentrations they behave as conventional electrolyte solutions, while at higher concentrations they behave like an expanded ("lubricated") IL. The transition region ($x_{IL} \approx 0.2$) is characterized by redissociation of the ion pairs and establishment of an IL-like structure.

■ ASSOCIATED CONTENT

Supporting Information

Tables of additional densities and electrical conductivities for [bmim][BF_4]; dielectric relaxation parameters (S_j, τ_j, α_1) of the D+CC+D model for [emim][BF_4], [bmim][BF_4], and [hmim]-[BF_4]; parameters of eq 5; figures. This material is available free of charge via the Internet at http://pubs.acs.org.

■ AUTHOR INFORMATION

Corresponding Author

*E-mail: Richard.Buchner@chemie.uni-regensburg.de.

Notes

The authors declare no competing financial interest.

■ ACKNOWLEDGMENTS

The authors thank Prof. M. Bešter-Rogač for communicating association constants of her conductivity measurements prior to publication and Prof. W. Kunz for the provision of laboratory facilities. This work was funded by the Deutsche Forschungsgemeinschaft within Priority Program 1191.

■ REFERENCES

(1) Wasserscheid, P.; Welton, T. *Ionic Liquids in Synthesis*; Wiley-VCH: Weinheim, Germany, 2003.
(2) Pârvulescu, V. I.; Hardacre, C. *Chem. Rev.* **2007**, *107*, 2615.
(3) Martins, M. A, P.; Frizzo, C. P.; Moreira, D. N.; Zanatta, N.; Bonacorso, H. G. *Chem. Rev.* **2008**, *108*, 2015.
(4) Pinkert, A.; Marsh, K. N.; Pang, S.; Staiger, M. P. *Chem. Rev.* **2009**, *109*, 6712.
(5) Castner, E. W.; Wishart, J. F. *J. Chem. Phys.* **2010**, *132*, 120901.
(6) Wu, X.; Liu, Z.; Huang, S.; Wang, W. *Phys. Chem. Chem. Phys.* **2005**, *7*, 2771.
(7) Schrödle, S.; Annat, G.; MacFarlane, D. R.; Forsyth, M.; Buchner, R.; Hefter, G. *Chem. Commun.* **2006**, 1748.
(8) Canongia Lopes, J. N.; Costa Gomes, M. F.; Pádua, A. A. H. *J. Phys. Chem. B* **2006**, *110*, 16816.
(9) Pádua, A. A. H.; Costa Gomes, M. F.; Canongia Lopes, J. N. A. *Acc. Chem. Res.* **2007**, *40*, 1087.
(10) Katoh, R.; Hara, M.; Tsuzuki, S. *J. Phys. Chem. B* **2008**, *112*, 15426.
(11) Hunger, J.; Stoppa, A.; Hefter, G.; Buchner, R. *J. Phys. Chem. B* **2008**, *112*, 12913.
(12) Hunger, J.; Stoppa, A.; Hefter, G.; Buchner, R. *J. Phys. Chem. B* **2009**, *113*, 9527.
(13) Stoppa, A. Ph.D. Thesis, University of Regensburg, 2010.
(14) Parker, A. J. *Pure Appl. Chem.* **1981**, *53*, 1437.
(15) Chu, A.; Braatz, P. *J. Power Sources* **2002**, *112*, 236.
(16) Snyder, L. R.; Kirkland, J. J.; Dolan, J. W. *Introduction to Modern Liquid Chromatography*; Wiley: Hoboken, NJ, 2010.
(17) Barthel, J.; Neueder, R.; Schröder, P. *Electrolyte Data Collection, Part 1c: Conductivities, Transference Numbers, and Limiting Ionic Conducivities of Solutions of Aprotic, Protophobic Solvents I: Nitriles*; Dechema: Frankfurt am Main, Germany, 1996.
(18) Marcus, Y. *Ion Properties*; Marcel Dekker: New York, 1997.
(19) Aliotta, F.; Ponterio, R. C.; Saija, F.; Salvato, G.; Triolo, A. *J. Phys. Chem. B* **2007**, *111*, 10202.
(20) Mellein, B. R.; Aki, S. N. V. K.; Ladewski, R. L.; Brennecke, J. F. *J. Phys. Chem. B* **2007**, *111*, 131.
(21) Kremer, F.; Schönhals, A. *Broadband Dielectric Spectroscopy*; Springer: Berlin, 2003.
(22) Buchner, R.; Hefter, G. *Phys. Chem. Chem. Phys.* **2009**, *11*, 8984.

(23) Marcus, Y.; Hefter, G. *Chem. Rev.* **2006**, *106*, 4585.
(24) Buchner, R. *Pure Appl. Chem.* **2008**, *80*, 1239.
(25) Fraser, K. J.; Izgorodina, E. I.; Forsyth, M.; Scott, J. L.; MacFarlane, D. R. *Chem. Commun.* **2007**, 3817.
(26) Sangoro, J.; Iacob, C.; Serghei, A.; Naumov, S.; Galvosas, P.; Karger, J.; Wespe, C.; Bordusa, F.; Stoppa, A.; Hunger, J.; Buchner, R.; Kremer, F. *J. Chem. Phys.* **2008**, *128*, 214509.
(27) Umebayashi, Y; Jiang, J. C.; Lin, K. H.; Shan, Y. L.; Fuji, K.; Seki, S.; Ishiguro, S.; Lin, S. H.; Chang, H. C. *J. Chem. Phys.* **2009**, *131*, 234502.
(28) Maroncelli, M.; Zhang, X. X.; Liang, M.; Roy, D.; Ernsting, N. P. *Faraday Discuss. Chem. Soc.* **2012**, *154*, 409.
(29) Stoppa, A.; Hunger, J.; Buchner, R. *J. Chem. Eng. Data* **2009**, *54*, 472.
(30) (a) Böttcher, C. F. J. *Theory of Electric Polarization*; Elsevier: Amsterdam, 1973; Vol. *1*. (b) Böttcher, C. F. J.; Bordewijk, P. *Theory of Electric Polarization*; Elsevier: Amsterdam, 1978; Vol. *2*.
(31) Stoppa, A.; Hunger, J.; Buchner, R.; Hefter, G.; Thoman, A.; Helm, H. *J. Phys. Chem. B* **2008**, *112*, 4854.
(32) Hunger, J.; Stoppa, A.; Schrödle, S.; Hefter, G.; Buchner, R. *ChemPhysChem* **2009**, *10*, 723.
(33) Buchner, R.; Hefter, G. T.; May, P. M. *J. Phys. Chem. A* **1999**, *103*, 1.
(34) Buchner, R.; Capewell, S. G.; Hefter, G. T.; May, P. M. *J. Phys. Chem. B* **1999**, *103*, 1185.
(35) Schrödle, S.; Hefter, G.; Kunz, W.; Buchner, R. *Langmuir* **2006**, *22*, 924.
(36) Barthel, J.; Bachhuber, K.; Buchner, R.; Hetzenauer, H.; Kleebauer, M. *Ber. Bunsenges. Phys. Chem* **1991**, *95*, 853.
(37) Barthel, J.; Buchner, R.; Eberspächer, P.-N.; Münsterer, M.; Stauber, J.; Wurm, B. *J. Mol. Liq.* **1998**, *78*, 82.
(38) Gregory, A. P.; Clarke, R. N. *Meas. Sci. Technol.* **2007**, *18*, 1372.
(39) Buchner, R.; Chen, T.; Hefter, G. T. *J. Phys. Chem. B* **2004**, *108*, 2365.
(40) Bevington, P. R. *Data Reduction and Error Analysis for the Physical Sciencies*; McGraw-Hill: New-York, 1969.
(41) Turton, D. A.; Hunger, J.; Stoppa, A.; Hefter, G.; Thoman, A.; Walther, M.; Buchner, R.; Wynne, K. *J. Am. Chem. Soc.* **2009**, *131*, 11140.
(42) Strictly speaking, such measurements should be corrected for solution viscosity. However, the required viscosities were unavailable for the present mixtures, with the exception of [bmim][BF_4] + AN.[43] Fortunately, the viscosity effect is rather small,[49] and below the experimental uncertainty in ρ ($\pm$0.05 kg m^{-3}) for almost all of the present mixtures. Accordingly, no viscosity corrections were made.
(43) Wang, J.; Tian, Y.; Zhao, Y.; Zhuo, K. *Green Chem.* **2003**, *5*, 618.
(44) Zafarani-Moattar, M. T.; Shekaari, H. *J. Chem. Thermodyn.* **2006**, *38*, 1377.
(45) Li, W.; Zhang, Z.; Han, B.; Hu, S.; Xie, Y.; Yang, G. *J. Phys. Chem. B* **2007**, *111*, 6452.
(46) Huo, Y.; Xia, S.; Ma, P. *J. Chem. Eng. Data* **2007**, *52*, 2077.
(47) Shekaari, H.; Zafarani-Moattar, M. T. *Int. J. Thermophys.* **2008**, *29*, 534.
(48) Chirico, R. D.; Diky, V.; Magee, J. W.; Frenkel, M.; Marsh, K. N.; Rossi, M. J.; McQuillan, A. J.; Lynden-Bell, R. M.; Brett, C. M. A.; Dymond, J. H.; Goldbeter, A.; Hou, J.-G.; Marquardt, R.; Sykes, B. D.; Yamanouchi, K.. *Pure Appl. Chem.* **2009**, *81*, 791.
(49) Heintz, A.; Klasen, D.; Lehmann, J. K.; Wertz, C. *J. Solution Chem.* **2005**, *34*, 1135.
(50) Ohba, T.; Ikawa, S. *Mol. Phys.* **1991**, *73*, 985.
(51) Stoppa, A.; Thoman, A.; Walther, M.; Buchner, R. Unpublished results.
(52) The relaxation time of the sub-α mode acts as the low-frequency cutoff for the relaxation time distribution of the dominating cation relaxation, which therefore shows physically realistic Debye behavior at long times.[41]
(53) Barthel, J.; Kleebauer, M.; Buchner, R. *J. Solution Chem.* **1995**, *24*, 1.
(54) Glarum, S. H. *J. Chem. Phys.* **1960**, *33*, 1371.
(55) Note that in refs 11, 12, and 32 the Powles–Glarum equation, eq 6, is given without the exponent $1/(1 - \alpha)$, which is correct only for calculating the rotational correlation time of a Debye process. Accordingly, the derived volumes of rotation, V_{eff}, are somewhat too large. However, the discussion in refs 11, 12, and 32 remains valid as the corrected V_{eff} values differ even more from the molecular volumes.
(56) Dote, J. C.; Kivelson, D.; Schwartz, R. N. *J. Chem. Phys.* **1981**, *85*, 2169.
(57) Dote, J. C.; Kivelson, D. *J. Phys. Chem.* **1983**, *87*, 3889.
(58) Wurm, B.; Münsterer, M.; Richardi, J.; Buchner, R.; Barthel, J. *J. Mol. Liq.* **2005**, *119*, 97.
(59) Cavell, E. A. S.; Knight, P. C.; Sheikh, M. A. *Trans. Faraday Soc.* **1971**, *67*, 2225.
(60) In contrast to the well-known Kirkwood correlation factor, g_K, which describes dipole–dipole correlations in neat dipolar fluids and which can be derived from statistical mechanics,[30] the present g_j values may also incorporate cross correlations among different dipolar species in the mixture.[32]
(61) Clare, B.; Hefter, G.; Singh, P. *Aust. J. Chem.* **1990**, *43*, 257.
(62) This value was adopted by assuming that $\Delta S_2 = 2 \times \sigma_{fit}$ of a fifth-order polynomial fitted to S_2 for $x_{IL} < 0.4$ with a fixed intercept of $S_2(0) = 32.51$.
(63) Shim, Y.; Kim, H. J. *J. Phys. Chem. B* **2008**, *112*, 11028.
(64) Roy, D.; Patel, N.; Conte, S.; Maroncelli, M. *J. Phys. Chem. B* **2010**, *114*, 8410.
(65) Huang, M.-M.; Bulut, S.; Krossing, I.; Weingärtner, H. *J. Chem. Phys.* **2010**, *133*, 101101.
(66) Semiempirical calculations of various confomers were performed using MOPAC2009[80] and the PM6 Hamiltonian. Dipole moments were calculated assuming the geometric center as the pivot. Molecular diameters were obtained by taking the longest distance between two atoms and adding the van der Waals radii of those atoms.[81] These diameters were used to calculate the maximum molecular volumes. To mimic solvent effects, the COSMO technique was applied assuming the dielectric permittivity of AN. Quantitative agreement with experimental values cannot be expected because of the known uncertainties arising from the combination of the PM6 Hamiltonian with the COSMO model for charged particles and low solvent permittivities. van der Waals volumes were determined from the optimized geometry with WINMOSTAR.[82]
(67) Canongia Lopes, J. N. A.; Pádua, A. A. H. *J. Phys. Chem. B* **2006**, *110*, 3330.
(68) Zahn, S.; Uhlig, F.; Thar, J.; Spickermann, C.; Kirchner, B. *Angew. Chem., Int. Ed.* **2008**, *47*, 3639.
(69) Gutman, V. *The Donor-Acceptor Approach to Molecular Interactions*; Plenum: New York, 1978.
(70) Chaban, V. A.; Prezhdo, O. V. *Phys. Chem. Chem. Phys.* **2011**, *13*, 19345.
(71) Jin, H.; O'Hare, B.; Dong, J.; Arzhantsev, S.; Baker, G. A.; Wishart, J. F.; Benesi, A. J.; Maroncelli, M. *J. Phys. Chem. B* **2008**, *112*, 81.
(72) Bockris, J. O'M.; Reddy, A. K. N. *Modern Electrochemistry: Ionics*; Plenum Press: New York, 1998; Vol. *1*.
(73) Bešter-Rogač, M.; Stoppa, A.; Hunger, J.; Buchner, R. *Phys. Chem. Chem. Phys.* **2011**, *13*, 17588.
(74) Katsuta, S.; Imai, K.; Kudo, Y.; Takeda, Y.; Seki, H.; Nakakoshi, M. *J. Chem. Eng. Data* **2008**, *53*, 1528.
(75) Bešter-Rogač, M. Unpublished results.
(76) The limited number of data points and their considerable scatter do not justify a better "fit" of $K_A(c_{IL})$. It should be kept in mind that the determination of K_A° from conductivity data also requires assumptions that can become important for weak association.[73]
(77) Barthel, J.; Iberl, L.; Rossmaier, J.; Gores, H. J.; Kaukal, B. *J. Solution Chem.* **1990**, *19*, 321.
(78) Barthel, J.; Kleebauer, M. *J. Solution Chem.* **1991**, *20*, 977.
(79) Wang, H.; Wang, J.; Zhang, S.; Pei, Y.; Zhuo, K. *ChemPhysChem* **2009**, *10*, 2516.
(80) Stewart, J. J. P. *MOPAC2009, version 9.097W ed.*; Stewart Computational Chemistry: Colorado Springs, CO, 2009.

(81) Bondi, A. *J. Phys. Chem.* **1964**, *68*, 441.
(82) Senda, N. Winmostar, version 3.78f (URL: http://winmostar.com/).